

Accepted Manuscript

Title: Comparative preclinical evaluation of ^{68}Ga -NODAGA and ^{68}Ga -HBED-CC conjugated procainamide in melanoma imaging

Authors: György Trencsényi, Noémi Dénes, Gábor Nagy, Adrienn Kis, András Vida, Flóra Farkas, Judit P. Szabó, Tünde Kovács, Ervin Berényi, Ildikó Garai, Péter Bai, János Hunyadi, István Kertész



PII: S0731-7085(17)30124-3
DOI: <http://dx.doi.org/doi:10.1016/j.jpba.2017.02.049>
Reference: PBA 11116

To appear in: *Journal of Pharmaceutical and Biomedical Analysis*

Received date: 13-1-2017
Revised date: 23-2-2017
Accepted date: 26-2-2017

Please cite this article as: György Trencsényi, Noémi Dénes, Gábor Nagy, Adrienn Kis, András Vida, Flóra Farkas, Judit P. Szabó, Tünde Kovács, Ervin Berényi, Ildikó Garai, Péter Bai, János Hunyadi, István Kertész, Comparative preclinical evaluation of ^{68}Ga -NODAGA and ^{68}Ga -HBED-CC conjugated procainamide in melanoma imaging, *Journal of Pharmaceutical and Biomedical Analysis* <http://dx.doi.org/10.1016/j.jpba.2017.02.049>

This is a PDF file of an unedited manuscript that has been accepted for publication. As a service to our customers we are providing this early version of the manuscript. The manuscript will undergo copyediting, typesetting, and review of the resulting proof before it is published in its final form. Please note that during the production process errors may be discovered which could affect the content, and all legal disclaimers that apply to the journal pertain.

Comparative preclinical evaluation of ^{68}Ga -NODAGA and ^{68}Ga -HBED-CC conjugated procainamide in melanoma imaging

György Trencsényi^{a,b,*}, Noémi Dénes^a, Gábor Nagy^b, Adrienn Kis^a, András Vida^{c,d}, Flóra Farkas^a, Judit P. Szabó^a, Tünde Kovács^{c,d}, Ervin Berényi^a, Ildikó Garai^b, Péter Bai^{c,d,e}, János Hunyadi^f, István Kertész^a

^aDepartment of Medical Imaging, Nuclear Medicine, University of Debrecen, Debrecen, Hungary;

^bScanomed LTD, Debrecen, Hungary;

^cDepartment of Medical Chemistry, University of Debrecen, Debrecen, Hungary;

^dMTA-DE Lendület Laboratory of Cellular Metabolism, Debrecen, Hungary;

^eResearch Center for Molecular Medicine, University of Debrecen, Hungary;

^fDepartment of Dermatology, University of Debrecen, Debrecen, Hungary.

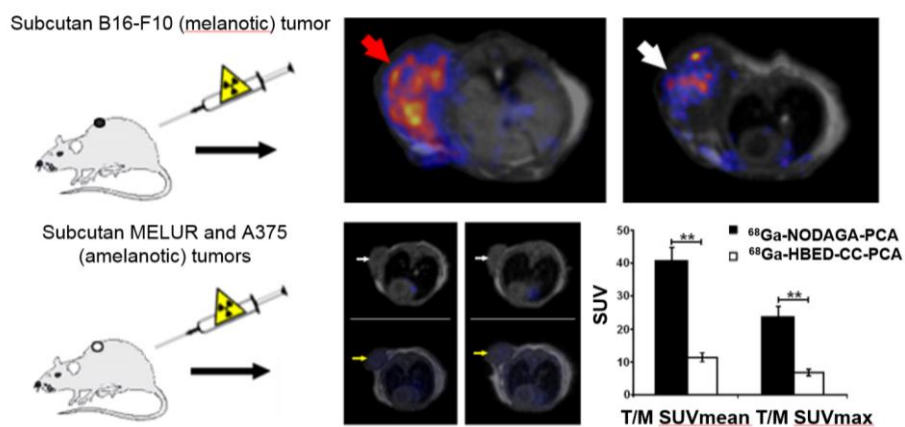
* corresponding author

Corresponding author:

György Trencsényi, PhD, University of Debrecen, Department of Medical Imaging, Nuclear Medicine, 4032, Debrecen, Nagyerdei krt. 98. Debrecen, Hungary,

E-mail: trencsenyi.gyorgy@med.unideb.hu

Graphical abstract



Highlights

- Radiolabeled benzamide derivatives can play an important role in melanoma imaging
- ^{68}Ga -labeled procainamide derivatives showed high melanin specificity
- Procainamide was conjugated with ^{68}Ga -labeled NODAGA and HBED-CC chelators
- Properties of the chelators determines the biological behaviour of the probe

Abstract

Malignant melanoma is the most aggressive form of skin cancer. The early detection of primary melanoma tumors and metastases using non-invasive PET imaging determines the outcome of this disease. Previous studies have shown that benzamide derivatives (e.g. procainamide) conjugated with PET radionuclides specifically bind to melanin pigment of melanoma tumors. ^{68}Ga chelating agents can have high influence on physiological properties of ^{68}Ga labeled bioactive molecules, as was experienced during the application of HBED-CC on PSMA ligand. The aim of this study was to assess this concept in the case of the melanin specific procainamide (PCA) and to compare the melanin specificity of ^{68}Ga -labeled PCA using HBED-CC and NODAGA chelators under *in vitro* and *in vivo* conditions.

Procainamide (PCA) was conjugated with HBED-CC and NODAGA chelators and was labeled with Ga-68. The melanin specificity of ^{68}Ga -HBED-CC-PCA and ^{68}Ga -NODAGA-PCA was investigated *in vitro* and *in vivo* using amelanotic (MELUR and A375) and melanin containing (B16-F10) melanoma cell lines. Tumor-bearing mice were prepared by subcutaneous injection of B16-F10, MELUR and A375 melanoma cells into C57BL/6 and SCID mice. 21±2 days after tumor cell inoculation and 90 min after intravenous injection of the ^{68}Ga -labelled radiopharmaceuticals whole body PET/MRI scans were performed.

^{68}Ga -NODAGA-PCA and ^{68}Ga -HBED-CC-PCA were produced with excellent radiochemical purity (98%). *In vitro* experiments demonstrated that after 30 and 90 min incubation time ^{68}Ga -NODAGA-PCA uptake of B16-F10 cells was significantly ($p\leq 0.01$) higher than the ^{68}Ga -HBED-CC-conjugated PCA accumulation in the same cell line. Furthermore, significant difference ($p\leq 0.01$ and 0.05) was found between the uptake of melanin negative and positive cell lines using ^{68}Ga -NODAGA-PCA and ^{68}Ga -HBED-CC-PCA. *In vivo* PET/MRI studies using tumor models revealed significantly ($p\leq 0.01$) higher ^{68}Ga -NODAGA-PCA uptake (SUVmean: 0.46 ± 0.05 , SUVmax: 1.96 ± 0.25 , T/M ratio: 40.7 ± 4.23) in B16-F10 tumors in contrast to ^{68}Ga -HBED-CC-PCA where the SUVmean, SUVmax and T/M ratio were 0.13 ± 0.01 , 0.56 ± 0.11 and 11.43 ± 1.24 , respectively.

Melanin specific PCA conjugated with NODAGA chelator showed higher specific binding properties than conjugated with HBED-CC. The chemical properties of the bifunctional chelators used for ^{68}Ga -labeling of PCA determine the biological behaviour of the probes. Due to the high specificity and sensitivity ^{68}Ga -labeled PCA molecules are promising radiotracers in melanoma imaging.

Abbreviations

BFC	bifunctional chelator
DIPEA	N,N-diisopropylethylamine
EDAC	N-(3-dimethylaminopropyl)-N'-ethylcarbodiimide hydrochloride
HBED-CC	N,N'-bis-[2-hydroxy-5-(carboxyethyl)benzyl]ethylenediamine-N,N'-diacetic acid
MeCN	acetonitrile
MRI	magnetic resonance imaging
NODAGA	1,4,7-triazacyclononane-1-glutaric acid-4,7-diacetic acid
PCA	procainamide (4-amino-N-(2-diethylaminoethyl)benzamide)
PET	positron emission tomography
PSMA	prostate-specific membrane antigen
RT	room temperature
TFA	trifluoroacetic acid

Keywords: ^{68}Ga , HBED-CC; Melanoma; NODAGA; Positron Emission Tomography, Procainamide

1. Introduction

Malignant melanoma is the most aggressive form of skin cancer and it is associated with high mortality [1]. The prognosis of patients with melanoma metastases is very poor. The five-year survival rate is between 5-19% when widespread metastatic lesions are present in several organs (*e.g.*: brain, liver, lung) largely reducing the length of patient survival [2]. Because of its high metastatic potential the early detection of small metastasis using high-resolution imaging techniques (*e.g.*: Positron Emission Tomography-PET; Magnetic Resonance Imaging-MRI) is critical in patient survival [3,4].

In routine clinical use 2-[¹⁸F] fluoro-2-deoxy-D-glucose (¹⁸FDG) is the most commonly used probe for PET imaging, however, ¹⁸FDG - as a biomarker of glucose metabolism - is not tumor- and hereby, not melanoma-specific [5]. Recently, several radiolabeled carrier molecules, such as melanoma-selective antibodies [6], α -MSH receptor ligands [7] and benzamide derivatives [8,9] have been tested for melanoma imaging and radiotherapy. As a potential target molecule melanin plays an important role in PET imaging of malignant melanoma. Due to its chemical structure polycyclic aromatic hydrocarbons and organic amines are capable of binding to melanin [10]. It has been shown that benzamide derivatives (*e.g.*: procainamide) specifically bind to melanin pigment, therefore several radiolabeled benzamide derivatives have been developed for molecular imaging of melanoma such as ⁶⁸Ga-SCN-DOTA-PCA, ⁶⁸Ga-SCN-NOTA-BZA [8,9] or [¹⁸F]N-(2-diethylaminoethyl)-4-[2-(2-(2-fluoroethoxy) ethoxy)ethoxy]benzamide ([¹⁸F]FPBZA) [11].

For monitoring malignancies or functional disorders, nuclear medicine applies different radionuclides. The most frequently used radionuclides for PET are cyclotron produced: ¹¹C ($t_{1/2} = 20$ min), ¹³N ($t_{1/2} = 10$ min), ¹⁵O ($t_{1/2} = 2$ min), and ¹⁸F ($t_{1/2} = 110$ min). These non-metallic radioisotopes are dominantly introduced into the biological carriers by means of covalent bonds. The other way for radiolabeling is the use of radiometals, such as ⁶⁴Cu, ⁶⁸Ga, and ⁸⁶Y. Among these radiometals ⁶⁸Ga ($t_{1/2} = 68$ min) is an outstanding radioisotope for molecular imaging due to its significant 89% positron yield. Moreover, ⁶⁸Ga is easily obtained from ⁶⁸Ge/⁶⁸Ga generator without the establishment of expensive cyclotron and synthesis facility [12].

The most common way of radiolabeling with radiometals (*e.g.*: ⁶⁸Ga) is the application of bifunctional chelators (BFCs) [13]. BFCs responsible for dual role, they have a reactive functional group to form stable covalent bond with the biological vector and they have a strong metal chelating property also. The first “universal” ligand for imaging applications was

the 1,4,7,10-tetraazacyclododecane-1,4,7,10-tetraacetic acid (DOTA) and it became one of the most popular macrocyclic chelators for the complexation of radiometals during the last decades [14]. However, in ^{68}Ga radiolabeling DOTA does not show ideal properties, for the effective complexation elevated temperature is essential. Triazacyclononane derivatives (e.g., 1,4,7-triazacyclononane-1,4,7-triacetic acid (NOTA) and 1,4,7-triazacyclononane-1-glutaric acid-4,7-diacetic acid (NODAGA)) provide a smaller coordination pocket and grant higher thermodynamic stability for gallium-complexes [14,15] and with these structures the labeling at room temperature is also an option [16].

Furthermore, among the open chain chelators N,N'-bis-[2-hydroxy-5-(carboxyethyl)benzyl]ethylenediamine-N,N'-diacetic acid (HBED-CC) is a highly effective chelator for ^{68}Ga -labeling, which has an extremely high thermodynamic stability constant [17]. The labeling conditions are mild due to the acyclic structure [18] and the given Ga-complex has high kinetic inertness at physiological pH [19] which is essential for in vivo applications. Nevertheless, recently it has been shown that the chelator-systems can play also the role of the pharmacokinetic modifier, the application of different BFC can affect the accumulation pattern also of the entire molecule [20]. Therefore, the aim of this study is to investigate the effect of HBED-CC-conjugation to a low-molecular weight compound procainamide (PCA) and to compare its radiochemical and biological properties with our existing NODAGA-conjugated analogue.

2. Materials and methods

2.1 Chemicals

For the ^{68}Ga labeling procedures: ACS grade water for ultratrace analysis – Sigma-Aldrich Kft. (Budapest, Hungary) – Ultrapur HCl and Suprapur NaOH*H₂O were purchased from Merck Kft. (Budapest, Hungary). HBED-CC-tris(tBu)ester was acquired from ABX GmbH (Germany, Radeberg). All other chemicals were the products of Sigma-Aldrich Kft. (Budapest, Hungary) and they were used without further purification.

2.2 Synthesis of HBED-CC-tris(tBu) tetra-fluoro-phenyl ester

70 mg (100 μmol) of N,N'-Bis[2-hydroxy-5-(carboxyethyl)-benzyl]ethylenediamine-N,N'-diacetic acid, tris tert-butyl ester (HBED-CC-tris(tBu)ester) was dissolved in 1 ml acetonitrile

(MeCN) and 20 mg (120 μmol) of 2,3,5,6-tetrafluorophenol, 23 mg (120 μmol) of N-(3-dimethylaminopropyl)-N'-ethylcarbodiimide hydrochloride (EDAC) and 50 μl (286 μmol) of N,N-diisopropylethylamine (DIPEA) were added. The mixture was stirred for 2 hours and then it was evaporated. The crude product was re-dissolved in 0.75 ml ethyl acetate and it was transferred into a silica chromatographic column (3 g solid phase). The column was rinsed with a mixture of ethyl acetate/ methanol (10:1) and the product was recovered with a mixture of ethyl acetate/ methanol (4:1). The combined organic phases were evaporated to get 68.3 mg of white solid (yield: 80.4%). The compound was reacted further as we received. $M_w = 849.42$ $[\text{M}+\text{H}]^+$.

2.3 Conjugation reaction of 4-amino-N-(2-diethylaminoethyl)benzamide hydrochloride with HBED-CC-tris(tBu)ester

13.6 mg (50 μmol) of 4-amino-N-(2-diethylaminoethyl)benzamide hydrochloride was dissolved in 1 ml of MeCN / 0.1 M sodium carbonate buffer (pH 9.5) 9:1 and 65 mg (75 μmol) of tetrafluorophenyl ester of HBED-CC-tris(tBu)ester was added to the solution. The pH of this mixture was adjusted to time to time between 8.5 and 9 by means of 2% NaOH solution during the whole procedure (24 hours, room temperature). After the completion of the reaction the solvent was evaporated in vacuum and the mixture was dissolved in 4 ml of 75% MeCN. For the cleavage of the -tBu protecting groups 2 ml of trifluoroacetic acid was added and the solution was stirred for 60 min and evaporated to dryness. The solid material was dissolved in water and was purified on a semi-preparative RP-HPLC. The collected fractions were lyophilized. Finally, a 3 mmol/dm³ of stock solution was prepared for the radiolabeling reactions. The product was characterized by ESI-MS (Shimadzu LCMS IT-TOF Mass Spectrometer, Shimadzu Corp., Tokyo, Japan) and ¹H-NMR (Bruker WP 360 SY).

2.4 Preparative and analytical RP-HPLC methods for the precursor

In order to purify the precursor HBED-CC-PCA, a KNAUER HPLC system with semi-preparative Supelco Discovery® Bio Wide Pore C18 column (150 mm x 10 mm; 10 μm diameters), and a flow rate of 4.4 ml/min was applied. The conditions of the separation were identical with the applied ones with NODAGA-PCA [21]. After a short isocratic period (3 min) a linear gradient was used (3 min 0% B; 20 min 50% B) with eluent A (0.1% TFA in

water) and eluent B (0.1% TFA in MeCN-H₂O (95:5, v/v), utilizing 254 nm for peak detection. For assessing the purity of the HBED-CC-PCA, a KNAUER HPLC was used. It was equipped with a Supelco Discovery® Bio Wide Pore C18 column (250 mm x 4.6 mm) 10 µm diameters, and 1.2 ml/min flow rate was applied, with a gradient profile: 0 min 2% B, 6 min 2% B; 30 min 40% B (mobile phases are identical than mentioned earlier). Signals were detected by UV detector (254 nm).

2.5 Radiolabeling of NODAGA-PCA and HBED-CC-PCA with ⁶⁸Ga

The labeling protocol were published earlier by Kertész et al. [21]. Briefly, the ⁶⁸Ga was eluted from the generator by using 0.1 M HCl, and fractional elution procedure was applied. 1 ml from the highest activity aliquot was buffered with sodium-acetate (1 M; 0.15 ml, aq.) and the pH of the mixture was adjusted to ~ 4.5 by the addition of sodium-hydroxide (2 %, 0.06 ml, aq.). Subsequently, 5 µl of a 3 mM NODAGA-PCA or HBED-CC-PCA stock-solution was introduced to the mixture and the reaction was incubated for 5 min at 95°C. After a short cooling period, the solution was transferred onto a preactivated Oasis HLB 1 cc cartridge, it was rinsed by 2 ml of water for injection. To eluate the activity from the column it was washed with 0.5 ml of isotonic NaCl solution/EtOH 2:1 mixture, and to decrease the alcohol content below 10% the solution was diluted further with 4 times more saline. Finally the solution was sterile filtered. The specific activities of the productions vary between 13-17 GBq/µmol. The radiochemical purity (%) of the final product was determined by application of an analytical RP-HPLC.

2.6 Determination of the radiochemical purity of ⁶⁸Ga-HBED-CC-PCA by analytical RP-HPLC

For the quality control of the ⁶⁸Ga-labelled radiopharmaceutical we used the identical system described as analytical HPLC, but equipped with a radiodetector. Signals were parallel detected by radiodetector and UV detector (254 nm).

2.7 Determination of partition coefficient of ⁶⁸Ga-HBED-CC-PCA

This protocol is based on the procedure described earlier [21]. Briefly, the partition coefficient was determined by mixing approximately 1.5 MBq of the ^{68}Ga -HBED-CC-PCA complex (10 μl) with a mixture of 500 μl of 1-octanol and 500 μl of PBS solution (pH 7.4) in a centrifuge tube. The mixture was shaken thoroughly for 20 minutes and then centrifuged at 20,000 rpm/min for 5 min for complete separation of the layers. Aliquots (100 μl) were taken from them and the samples were loaded into test tubes; the radioactivity was determined with a Perkin-Elmer Packard Cobra gamma counter.

2.8 Determination of *in vitro* stability of ^{68}Ga -HBED-CC-PCA

This protocol is based on the procedure described by Kertész et al. [21]. Shortly, the stability of ^{68}Ga -HBED-CC-PCA was tested in rat serum at 37°C. Approximately 8 MBq of ^{68}Ga -HBED-CC-PCA was introduced into mouse serum and was incubated. 50 μL aliquot from this mixture at different time points (0, 30, 60, 90 and 120 min) was combined with 50 μl cold abs. EtOH. Precipitated fraction was pelleted by centrifugation at 20,000 rpm for 5 min. The supernatant was collected, further diluted with water and the radiochemical purity of ^{68}Ga -HBED-CC-PCA was assessed by means of the analytical RP-HPLC.

2.9 Cell culture

Melanin-producing B16-F10 (mouse) and amelanotic A375 and MELUR (human) melanoma cell lines were purchased from the American Type Culture Collection (ATCC). B16-F10 cells were cultured in Dulbecco's Modified Eagle's medium (DMEM, GIBCO Life Technologies) supplemented with 1% (v/v) MEM Non Essential Amino Acid solution (Sigma-Aldrich), 1% MEM Vitamins solution (Sigma-Aldrich), 10% Fetal Bovine Serum (FBS, GIBCO Life technologies) and 1% Antibiotic and Antimicotic solution (Sigma-Aldrich). A375 and MELUR cells were cultured in Dulbecco's Modified Eagle's medium (DMEM, GIBCO Life Technologies) supplemented with 10% Fetal Bovine Serum (FBS, GIBCO Life technologies) and 1% Antibiotic and Antimicotic solution (SIGMA). All cell lines were cultured at regular conditions (5% CO_2 , 37 °C). For *in vitro* studies and tumor induction the cells were used at 80% confluence and the viability of the cells was always higher than 90%, as assessed by the trypan blue exclusion test.

2.10 *In vitro* saturation binding studies

For *in vitro* saturation binding studies melanotic B16-F10 cells were used. The cells were cultured in 24-well plates (5×10^4 per well) for 24 h. Different concentration (20-1600 nM) of ^{68}Ga -NODAGA-PCA or ^{68}Ga -HBED-CC-PCA was added to each well in 200 μl volume. After 1 hour incubation time (in CO_2 incubator at 37 °C) the medium was removed and the cells were washed twice with PBS, then washed twice with glycine (0.2 M) and lysed with NaOH (1M) for 10 min at 37 °C.

2.11 Cellular uptake and efflux studies

Method A: B16-F10, A375 and MELUR cells were grown as monolayer in tissue culture flasks (2×10^5 cells per T25 flask) for 24 h. 0.37 MBq of ^{68}Ga -NODAGA-PCA or ^{68}Ga -HBED-CC-PCA was then added to each flask and cells were further incubated for 30 and 90 min at 37 °C. After the incubation time cells were washed twice with PBS, trypsinized and the cell number was counted. The radioactivity was measured with gamma-counter (Cobra-II, Canberra Packard, USA) for 1 min within the ^{68}Ga -sensitive energy window and decay-corrected radiotracer uptake was expressed as counts min^{-1} (10^6 cells) $^{-1}$ (cpm). The percent uptake (% uptake) was calculated as the percent of the total added radioactivity found in the pellet. For the determination of ^{68}Ga -NODAGA-PCA and ^{68}Ga -HBED-CC-PCA efflux the cells growing in monolayer were first loaded with the radioligands (0.37 MBq at 37 °C for 30 and 90 min) then washed twice with PBS. Afterwards, 5 ml DMEM was added to each culture flask and the adherent cells were further incubated for 10 min at 37 °C without radioligands. After the incubation time cells were washed twice with PBS, trypsinized and the cell number was counted. The radioactivity was measured with gamma-counter.

Method B: B16-F10, A375 and MELUR cells were grown as monolayer for 24 h. Subsequently, cells were trypsinized, centrifuged and resuspended in DMEM and were aliquoted in test tubes at a cell concentration of $1 \times 10^6 \text{ ml}^{-1}$. Each tube was incubated for 30 and 90 min in the presence of 0.37 MBq ^{68}Ga -NODAGA-PCA or ^{68}Ga -HBED-CC-PCA at 37 °C. After the incubation time samples were washed 3 times with ice-cold PBS and the radioactivity was measured with gamma counter. For the efflux studies cells were first loaded with radioligands (0.37 MBq at 37 °C for 30 and 90 min). After the incubation time cells were

then washed PBS containing 1 mM glucose (gl-PBS) at room temperature. Subsequent centrifugation the supernatant was removed and the cells were resuspended in 2 ml gl-PBS and further incubated for 10 min at 37 °C without radioligands. The efflux was terminated by the addition of ice-cold PBS. The cells were then washed twice with ice cold PBS and the radioactivity was measured using gamma-counter.

2.12 *In vivo* tumor models

C57BL/6J and CB17 SCID mice were housed under sterile conditions at a temperature of $26\pm 2^\circ\text{C}$, with $50\pm 10\%$ humidity and artificial lighting with a circadian cycle of 12 h. Sterile semi-synthetic diet (Akronom Ltd., Budapest, Hungary) and sterile drinking water were available *ad libitum* to all the animals. Laboratory animals were kept and treated in compliance with all applicable sections of the Hungarian Laws and regulations of the European Union. For the induction of *in vivo* tumor models adult female CB17 SCID (n=30) and C57BL/6J (n=20) were used at 10 weeks of age. For the induction of amelanotic tumor models CB17 SCID mice were used; 1×10^5 amelanotic Melur or A375 tumor cells in 0.9% NaCl (100 μl) were injected into the left shoulder area. To generate melanotic melanoma tumors C57BL/6J mice were subcutaneously injected with B16-F10 tumor cells (1×10^5 in 100 μl saline) into the left shoulder area. The tumor size was assessed by caliper measurements and was calculated as follows: $(\text{largest diameter} \times \text{smallest diameter}^2)/2$. *In vivo* and *ex vivo* experiments were carried out 21 ± 2 days after subcutaneous injection of tumor cells at the tumor volume of $110\pm 10 \text{ mm}^3$.

2.13 Animal PET/MRI imaging

Control and tumor-bearing animals were injected with $10.3\pm 0.3 \text{ MBq}$ of ^{68}Ga -NODAGA-PCA or ^{68}Ga -HBED-CC-PCA *via* the lateral tail vein. 90 min after radiotracer injection mice were anaesthetized by 3% isoflurane (Forane) with a dedicated small animal anesthesia device and whole body PET scans (20-min static PET scans) were acquired using the preclinical *nanoScan* PET/MRI system (Mediso Ltd., Hungary). To prevent movement, animals were fixed into a mouse chamber (MultiCell Imaging Chamber, Mediso Ltd., Hungary) and positioned in the center of field of view (FOV). For the determination of the anatomical

localization of the organs and tissues, T1-weighted MRI scans were performed (3D GRE EXT multi-FOV; TR/TE 15/2 ms; FOV 40 mm; NEX 2). PET volumes were reconstructed using a three-dimensional Ordered Subsets Expectation Maximization (3D-OSEM) algorithm (Tera-Tomo, Mediso Ltd., Hungary). PET and MRI images were automatically co-registered by the acquisition software (Nucline) of *nanoScan* PET/MRI instrument. Images were analyzed with the InterView™ FUSION (MedisoLtd., Hungary) dedicated image analysis software. Radiotracer uptake was expressed in terms of standardized uptake values (SUVs). Ellipsoidal 3-dimensional Volumes of Interest (VOI) were manually drawn around the edge of the tissue or organ activity by visual inspection using InterView™ FUSION multi-modal visualization and evaluation software (Mediso Ltd., Hungary). The standardized uptake value (SUV) was calculated as follows: $SUV = [VOI \text{ activity (Bq/mL)}] / [\text{injected activity (Bq)} / \text{animal weight (g)}]$, assuming a density of 1 g/mL. Tumor-to-muscle (T/M) ratios were computed as the ratio between the activity in the tumor VOI and in the background (muscle) VOI.

2.14 *Ex vivo* biodistribution studies

One day after *in vivo* PET/MRI imaging animals were injected intravenously with 10.3 ± 0.3 MBq of ^{68}Ga -NODAGA-PCA or ^{68}Ga -HBED-CC-PCA. Mice were euthanized 90 min after the injection of ^{68}Ga -labeled tracers with 5% isoflurane. Tissue samples were taken from each organ and their weight and radioactivities were measured with gamma counter and DAR (Differential Absorption Ratio) values were calculated ($[\text{accumulated radioactivity/g tissue}] / [\text{total injected radioactivity/body weight}]$).

2.15 Statistical analysis

Significance was calculated by Mann-Whitney U-test and the significance level was set at $p \leq 0.05$ unless otherwise indicated. Data are presented as mean \pm SD of at least three independent experiments.

3. Results

3.1 Chemical and radiochemical synthesis

HBED-CC-PCA was prepared by a conjugation of 4-amino-N-(2-diethylaminoethyl)benzamide hydrochloride and HBED-CC-tris(tBu)-ester (Fig 1.) and a subsequent protecting group removal. The final product was purified by semi-preparative RP-HPLC. The purity of HBED-CC-PCA was checked by analytical HPLC, and it proved to be better than 98%. The chemical structure of the product was assessed by $^1\text{H-NMR}$ and ESI-MS. The purified product was identified by ESI-MS: $M_w=750.37$ $[\text{M}+\text{H}]^+$. $^1\text{H-NMR}$ (DMSO d_6) δ = (1-1.07 (t, 6H), 2.5-2.7 (m, 8H), 2.78-2.97 (m, 10H), (3.55-3.63 (m, 6H), 4.12-4.25 (m, 4H), 6.7-6.75 (m, 2H), 6.8-6.85 (m, 2H), 6.95-7 (m, 4H), 7.65-7.75 (m, 2H). We have performed a manual protocol for radiolabeling and the overall reaction time of producing $^{68}\text{Ga-HBED-CC-PCA}$ was 15 min. including the reformulation step also. The decay corrected yield was $65.87\pm 8.25\%$ ($n=7$) and the radiochemical purity was at least 98%. The retention factor of the active compound was 9.5 min. The specific activity of the product was 14.81 ± 1.71 GBq/ μmol . The quality control measurements demonstrated that in the final product all of the isomers exist in different ratios.

3.2 Partition coefficient and *in vitro* stability of $^{68}\text{Ga-HBED-CC-PCA}$

The partition coefficient ($\log P$) of $^{68}\text{Ga-HBED-CC-PCA}$ was determined to be -2.19 ± 0.12 . In comparison with the $^{68}\text{Ga-NODAGA-PCA}$ (-2.79 ± 0.10 ; [21]) it means that the new compound has a bit higher lipophilicity, but the compound is still hydrophilic. Furthermore, in order to measure the stability of the newly labeled compound in mouse serum at 37 °C, analytical radio-HPLC was used. After 2 hours of incubation in mouse serum, approximately 75% of the original compound was found intact.

3.3 *In vitro* studies

In vitro saturation binding studies showed a positive correlation between the concentration of $^{68}\text{Ga-NODAGA-PCA}$ and its binding using B16-F10 cells (Fig. 2A). Similar correlation was found using $^{68}\text{Ga-HBED-CC}$ conjugated PCA, but significantly lower binding was observed (Fig. 2B). The melanin specificity of $^{68}\text{Ga-NODAGA-PCA}$ and $^{68}\text{Ga-HBED-CC-PCA}$ was investigated using melanotic B16-F10 and amelanotic A375 and Melur cell lines. Cellular

uptake and efflux was investigated using melanoma cells in suspension and in monolayer (see Materials and methods: Method A and B in Cellular uptake and efflux studies). In suspension (using Method A) the accumulation of ^{68}Ga -NODAGA-PCA and ^{68}Ga -HBED-CC-PCA in B16-F10 cells were significantly higher ($p<0.05$ and $p<0.01$) than in amelanotic A375 or Melur cells at each time point (Fig. 2C, D). In experiments where the cellular uptake of the two melanin specific radiotracer was compared, we found that ^{68}Ga -NODAGA-PCA accumulation in B16-F10 cells was significantly higher ($p<0.001$) (1.56 ± 0.39 at 30 min; 2.58 ± 0.69 at 90 min) than the accumulation of ^{68}Ga -HBED-CC-PCA (0.06 ± 0.017 at 30 min; 0.17 ± 0.03 at 90 min). Similar results were found when plated cells were used (Method B) for the determination of the melanin specificity of the two radiolabeled compounds (Fig. 2E, F). When melanoma cells in monolayer were used for cellular uptake studies, we found significantly higher ($p<0.01$) ^{68}Ga -NODAGA-PCA accumulation in melanin containing B16-F10 cells (1.97 ± 0.44 at 30 min; 3.61 ± 0.46 at 90 min) than in amelanotic A375 (0.30 ± 0.09 at 30 min; 0.27 ± 0.18 at 90 min) or Melur (0.18 ± 0.07 at 30 min; 0.31 ± 0.24 at 90 min) cells. In melanotic B16-F10 cells the ^{68}Ga -NODAGA-PCA accumulation was approximately seven-fold higher at each time point than the ^{68}Ga -HBED-CC-PCA uptake confirming the higher melanin specificity of the NODAGA chelator containing radiotracer. In addition, relatively higher ^{68}Ga -NODAGA-PCA and ^{68}Ga -HBED-CC-PCA accumulation was observed using melanoma cells in monolayer than in suspension.

In washout (efflux) experiments cells were first loaded with ^{68}Ga -NODAGA-PCA or ^{68}Ga -HBED-CC-PCA, and after extensive washing rounds the cells were further incubated for 10 min without radioactivity. Using this method both in suspension and monolayer significant ($p\leq 0.01$) differences were found between the ^{68}Ga -NODAGA-PCA accumulation of melanin positive and negative cell lines (Fig. 2C, E). Despite the lower uptake of ^{68}Ga -HBED-CC-PCA in melanoma cells, in efflux studies the melanin-containing B16-F10 cell line showed significantly ($p\leq 0.05$) higher ^{68}Ga -HBED-CC-PCA content at each time point than the melanin negative A375 and Melur cell lines both in suspension (Fig. 2D) and in monolayer (Fig. 2F) confirming the melanin specificity of ^{68}Ga -HBED-CC-PCA.

3.4 Biodistribution studies in control mice

Whole body PET/MRI imaging and *ex vivo* organ distribution studies were performed 90 min after intravenous injection of 10.3 ± 0.3 MBq ^{68}Ga -NODAGA-PCA or ^{68}Ga -HBED-CC-PCA using healthy C57BL/6 mice. Representative coronal PET/MRI images are shown in Fig. 3. By the qualitative analysis of PET images the urinary system (kidneys and urine) were clearly visualized. Low radiotracer accumulation was observed in the abdominal and thoracic regions using both radiotracers after 90 min incubation time (Fig. 3).

In vivo PET/MRI organ distribution results correlated well with the *ex vivo* data shown in Fig. 3C. For *ex vivo* distribution studies healthy control animals were sacrificed 90 min after radiotracer injection, and after dissection the accumulated activities of the organs and tissues were assessed by gamma counter. By the quantitative analysis no significant differences were found between the DAR values of organs and tissues when ^{68}Ga -NODAGA-PCA and ^{68}Ga -HBED-CC-PCA uptake were compared (Fig 3C). Remarkable accumulation was observed in kidneys (approx. DAR: 0.2-0.5) and urine (approx. DAR: 44-55) using both radiotracers. In contrast, slight radiotracer uptake was measured with low DAR values in the brain (0.02 ± 0.01), liver (0.05 ± 0.02), intestines (0.04 ± 0.01), spleen (0.03 ± 0.01), lung (0.02 ± 0.01) and muscle (0.01 ± 0.008) using ^{68}Ga -NODAGA-PCA. Relatively lower accumulation was found in the brain (0.01 ± 0.007), liver (0.02 ± 0.01), intestines (0.03 ± 0.01), spleen (0.01 ± 0.008), lung (0.01 ± 0.008) and muscle (0.01 ± 0.006) when the distribution of ^{68}Ga -HBED-CC-PCA was assessed.

3.5 PET/MRI imaging and *ex vivo* biodistribution studies of tumor-bearing mice

For the *in vivo* assessment of the melanin specificity of the Ga-68 labeled PCA tracers B16-F10, A375 and MELUR tumor-bearing animals were injected intravenously with 10.3 ± 0.3 MBq of ^{68}Ga -NODAGA-PCA or ^{68}Ga -HBED-CC-PCA and after 90 min incubation time whole body PET scans were acquired using the preclinical PET/MRI system. Representative whole body coronal and axial PET/MRI image of B16-F10 melanoma tumors are shown in Fig. 4. By the qualitative analysis of the PET/MRI images the subcutaneously growing B16-F10 tumors were clearly visualized with ^{68}Ga -NODAGA-PCA 90 min after the tracer injection (Fig. 4A, red arrows). After the quantitative analysis of PET images significant differences ($p \leq 0.01$ level) were found between the ^{68}Ga -NODAGA-PCA (SUVmean: 0.46 ± 0.05 , SUVmax: 1.93 ± 0.25) and ^{68}Ga -HBED-CC-PCA (SUVmean: 0.13 ± 0.01 , SUVmax: 0.56 ± 0.11) accumulation in the melanin positive B16-F10 tumors (Fig. 4C). In addition, when the ^{68}Ga -NODAGA-PCA uptake of B16-F10 tumors was compared to the muscle

(background) activity, we found that T/M SUV_{mean} and T/M SUV_{max} were 40.7 ± 4.23 and 23.55 ± 3.45 , respectively. These T/M SUV values were approximately four-fold higher than that of the ^{68}Ga -HBED-CC-PCA uptake ratios, where the T/M SUV_{mean} and T/M SUV_{max} values were 11.43 ± 1.24 and 6.82 ± 0.96 , respectively (Fig. 4D).

In contrast, very low ^{68}Ga -NODAGA-PCA and ^{68}Ga -HBED-CC-PCA uptake was observed when subcutaneous melanin negative tumors (MELUR, A375) were investigated using PET/MRI imaging system (Fig. 5). By the quantitative analysis of PET images we found that the SUV values (Fig. 5E) and tumor-to-muscle ratios (Fig. 5F) of negative tumors were significantly ($p \leq 0.01$) lower than of the B16-F10 tumors. Furthermore, no significant differences were found between the accumulation of ^{68}Ga -NODAGA-PCA and ^{68}Ga -HBED-CC-PCA radiopharmaceuticals in MELUR and A375 tumors.

For the investigation of melanin specificity of ^{68}Ga -NODAGA-PCA and ^{68}Ga -HBED-CC-PCA *ex vivo* biodistribution studies were performed 90 min post injection using subcutaneously growing B16-F10 and amelanotic A375 and Melur tumors. Table 1 demonstrates that the ^{68}Ga -NODAGA-PCA uptake of B16-F10 tumor was significantly ($p \leq 0.01$ (**)) higher than that of A375 or Melur tumors, confirming the melanin binding specificity of the ^{68}Ga -NODAGA-PCA *ex vivo*. By analyzing the tumor-to-muscle ratios, the difference between the B16-F10 and amelanotic tumors was also significant at $p \leq 0.01$. ^{68}Ga -HBED-CC-PCA showed significantly ($p \leq 0.05$ (*)) higher uptake in melanin positive B16-F10 tumors than in amelanotic tumors, however the accumulation of ^{68}Ga -HBED-CC-PCA in melanoma cell lines was lower when DAR values were compared to DAR values of ^{68}Ga -NODAGA-PCA.

4. Discussion

The most aggressive form of skin cancer is malignant melanoma. Considering that this malignancy is associated with high mortality, furthermore the prognosis of patients with metastases is very poor, hence the early detection of small metastatic lesions using high-resolution non-invasive imaging techniques (e.g.: PET) is critical in patient survival [11]. Among radionuclides used in PET, the cyclotron independent radionuclide ^{68}Ga offers a well-established chemistry for the labeling of small molar-weight biomolecules and peptides [22-

24]. ^{68}Ga -labeled procainamide shows great potential for diagnosis in a variety of melanomas producing melanin pigment. Here we described the radiosynthesis of the melanin specific ^{68}Ga -labeled HBED-CC-4-Amino-N-(2-diethylaminoethyl)benzamide (^{68}Ga -HBED-CC-PCA) and compared the preclinical evaluation of this product with our existing NODAGA-conjugated analogue ^{68}Ga -NODAGA-PCA [21].

The radiosynthesis of the melanin specific ^{68}Ga -HBED-CC labeled PCA was very similar to our previously described radiotracer ^{68}Ga -NODAGA-PCA [21]. The quality control measurements confirm that both of the compounds can be produced in the required radiochemical purity (98%), and due to the similar decay corrected yields (approx. 65-68) between the two melanin specific radiotracer the specific activities are also close together (approx. 13-17 GBq/ μmol). The overall reaction time of producing ^{68}Ga -HBED-CC-PCA was also 15 min. including the reformulation step. Therefore, this synthesis method enables us to produce the ^{68}Ga -HBED-CC-PCA for preclinical applications fast and easily with high radiochemical purity and specific activity. Furthermore, after 2 hours of incubation in mouse serum, still 75% of the original compound was found intact. Interestingly, this finding does not support the experience of Eder et al. [25] that the application of HBED-CC- vs. NODAGA can increase the metabolic stability of the radiotracer but the current compound is still a highly stable molecule, suitable for biological experiments.

For the investigation of the effect of using different chelators on the melanin specificity of ^{68}Ga -labeled PCA probes melanin positive B16-F10 and melanin negative melanoma cell lines (MELUR, A375) were used both in monolayer and in suspension (Fig. 2). Previous studies showed that transport processes (uptake/efflux) are different when cells are used in monolayer or in suspension for *in vitro* investigations [26,27]. We also found differences between the uptake of the melanin specific radiotracers when the suspension technique (Fig. 2C, D) was compared to the monolayer technique (Fig. 2E, F). Relatively higher ^{68}Ga -NODAGA-PCA and ^{68}Ga -HBED-CC-PCA accumulation was found at each time point when melanoma cells were used as monolayer. From these *in vitro* data we concluded that monolayer form is more physiological for the adherent melanoma cells. When the uptake of ^{68}Ga -HBED-CC-PCA was investigated using both *in vitro* methods (Fig. 2D, F), we found significantly ($p \leq 0.05$ and $p \leq 0.01$) higher accumulation in melanin producing B16-F10 cell than in melanin negative MELUR or A375 cells, furthermore, this accumulation increased with time and remained after 10 min efflux. Despite the low accumulation, these uptake results confirmed the melanin specificity of ^{68}Ga -HBED-CC-PCA. Previous studies also showed [8,9], that ^{68}Ga -labeled benzamide derivatives (^{68}Ga -SCN-NOTA-BZA and ^{68}Ga -

SCN-DOTA-PCA) specifically bind to melanin in B16-F10 melanoma cells and this accumulation increased in a time-dependent manner. As our research group and others reported earlier [9, 21,28-30] the uptake of ^{68}Ga -labeled procainamide is mediated by passive diffusion and the $\log P$ value of the labeled compounds plays an important role in this process. The $\log P$ of ^{68}Ga -HBED-CC-PCA was -2.19 ± 0.12 . In comparison with the ^{68}Ga -NODAGA-PCA ($\log P$ -2.79 ± 0.10) it means that the new compound has a bit stronger lipophilic character, but it is still highly hydrophilic.

As it was expected from the $\log P$ value and from the size of the ^{68}Ga -HBED-CC-PCA in biodistribution studies using healthy mice we found that ^{68}Ga -HBED-CC-PCA – similarly to the NODAGA conjugated PCA [21] – mainly excreted from the urinary system and low accumulation was observed in other organs and tissues after 90 min incubation time (Fig. 3). These *in vivo* and *ex vivo* results correlated well with several studies [8,9,11,28,31] where the biodistribution of other radiolabeled (^{18}F , ^{68}Ga , ^{125}I) benzamide derivatives were investigated.

The melanoma specificity of ^{68}Ga -HBED-CC-PCA was investigated by subcutaneous melanoma tumor-bearing mouse models and its biodistribution was compared with that of ^{68}Ga -NODAGA-PCA. Melanotic B16-F10 (in C57BL/6 mice) and amelanotic A375, Melur tumors (in SCID mice) were investigated 21 ± 2 days after tumor cell inoculation and 20-min static PET/MRI images were obtained 90 min after the *i.v.* injection of the radiotracers. The melanin containing B16-F10 tumors were clearly visualized by PET/MRI imaging with low background accumulation using both radiotracers (Fig. 4A, B). In contrast, when amelanotic MELUR (Fig. 5A, B) and A375 (Fig. 5C, D) tumors were used for PET imaging, very low ^{68}Ga -HBED-CC-PCA and ^{68}Ga -NODAGA-PCA accumulation was found confirming the melanin specificity of the radiotracers. After the quantitative SUV analysis of *in vivo* PET/MRI images and analyzing the *ex vivo* DAR (Table 1.) data, we found that ^{68}Ga -HBED-CC-PCA and ^{68}Ga -NODAGA-PCA uptake in melanotic B16-F10 tumor (Fig. 4C, D) was significantly ($p\leq 0.01$) higher than in amelanotic MELUR or A375 tumors (Fig. 5E, F). Our *in vivo* and *ex vivo* data correlated well with other research papers, where ^{18}F - and ^{68}Ga -labeled melanin specific benzamide derivatives were investigated and relatively high accumulation was found in melanin containing B16 tumors with excellent tumor-to-background contrast [8,9,11,28,31]. Despite the moderate accumulation of ^{68}Ga -HBED-CC-PCA (SUVmean: 0.13 ± 0.01 , SUVmax: 0.56 ± 0.11) and ^{68}Ga -NODAGA-PCA (SUVmean: 0.46 ± 0.06 , SUVmax: 1.93 ± 0.25) in subcutaneously growing B16-F10 tumors, we found that the low activity of other tissues allows of high quality images with high contrast. In addition, our molecules produced higher tumor-to-muscle ratios (T/M SUVmean of ^{68}Ga -NODAGA-PCA and ^{68}Ga -

HBED-CC-PCA was 40.7 ± 4.23 and 11.43 ± 1.24 , respectively) than ^{68}Ga -SCN-DOTA-PCA (9.47 ± 2.36) with a similar chemical structure what was synthesized by [9].

In this paper significant differences were found between the *in vitro*, *ex vivo* and *in vivo* accumulation of ^{68}Ga -NODAGA-PCA and ^{68}Ga -HBED-CC-PCA molecules. Overall, from our data we concluded that procainamide molecule is highly melanin specific, however, the properties of the used bifunctional chelator (BFC) determines the accumulation of the labeled compound in melanin positive melanoma cells and tumors. From an ideal BFC can expect the following properties: - fast complexation at a very low ion-concentration range, preferably at room temperature, - tolerance of a broad pH range, - and selectivity against the endogenous metal ions (Ca or Zn) or potential impurities originated from the production of the radionuclide (Fe or Al) [13,32]. The final radiolabeled compound should be resistant of the challenge of different endogenous ligands, such as transferrin or lactoferrin [33]. Therefore, the selection of the appropriate chelator is largely dependent on the applied isotope. A huge number of macrocyclic and open chain BFCs have been developed and tested in regard to satisfy the specific requirements mentioned earlier and several modifications were taken in geometries, donor atoms, pendant arms or coordination numbers [14,23,34]. The application of acyclic chelators (*e.g.* HBED-CC) usually grant fast complexation kinetics, but the kinetically inertness of these complexes usually not so high in comparison with the macrocyclic ones (*e.g.* NODAGA) [35,36]. Taking into account that the chelator-systems can play also the role of the pharmacokinetic modifier, the application of different BFC can affect the accumulation pattern also of the entire molecule, as the acyclic complexing agent HBED-CC coupled into a PSMA (prostate-specific membrane antigen) inhibitor, can influence the biological properties of the adduct in a positive way. On the other hand a possible drawback in comparison with other clinically approved chelators (*e.g.* NODAGA) can be that HBED-CC forms three diastereoisomers during gallium complexation. The ratio of the formed isomers depends on the temperature, the pH and the chelator concentration during the complexation reaction [33]. It was recently reported that during the standard labelling protocol, [^{68}Ga]-PSMA-HBED-CC (pH~4, temperature 95°C) mainly the thermodynamically favored diastereoisomer was formed; but measurable amount of the other isomers - due to the problematic separation - can be found in the final formulation prepared for the patient [25]. This feature can be the main limitation factor before the extensive application of HBED-CC in preclinical practice, because it has big importance to determine the exact biological activities of the diastereoisomers [25]. Therefore one can conclude that for biological application the selection of BFC depends on a certain threshold of termodinamical stability and

kinetic inertness, but after reaching them the main emphasis shift to the ideal pharmacokinetic properties and the preferably uniform product.

5. Conclusion

In this present study, we compared the synthesis and biological properties of the melanin specific ^{68}Ga -PCA molecule conjugated with HBED-CC and NODAGA chelators. It became clear that at this region of $\log P$ the hydrophilic-lipophilic balance will not predict correctly the transport of the radioligands across the cell membrane and the ligand-binding capacity of the melanin. Therefore, in the melanin producing experimental B16-F10 melanoma tumors the ^{68}Ga -labeled-PCA conjugated with NODAGA chelator showed higher binding properties with excellent imaging contrast. In conclusion, the present preclinical data has demonstrated a significant difference in the influence of different chelators for ^{68}Ga -PCA. This result should be taken into account during the development of ^{68}Ga -labeled melanoma specific probes for PET imaging.

Conflicts of interest statement

We declare that we have no conflict of interest.

Acknowledgements

This work was supported by a Bolyai fellowship to GT. Furthermore, by grants from the University of Debrecen, NKFIH (K108308, GINOP-2.3.2-15-2016-00006), the Momentum fellowship of the Hungarian Academy of Sciences and the University of Debrecen. The project is co-financed by the European Union and the European Regional Development Fund. The authors are sincerely grateful to Stephanie C. Fox, J.D. for her hard work in formatting, and editing this article.

References

- [1] A. Uong, L.I. Zon, Melanocytes in development and cancer, *J. Cell Physiol.* 222 (2010) 38-41.
- [2] A. Sandru, S. Voinea, E. Panaitescu, A. Blidaru, Survival rates of patients with metastatic malignant melanoma, *J. Med. Life.* 7 (2014) 572-576.
- [3] J. McIvor, T. Siew, A. Campbell, M. McCarthy, FDG PET in early stage cutaneous malignant melanoma, *J. Med. Imaging Radiat. Oncol.* 58 (2014) 149-154.
- [4] A.M. Rodriguez Rivera, H. Alabbas, A. Ramjaun, Value of positron emission tomography scan in stage III cutaneous melanoma: a systematic review and meta-analysis, *Surg. Oncol.* 23 (2014) 11-16.
- [5] L. Jiang, Y. Tu, H. Shi, Z. Cheng, PET probes beyond (18)F-FDG, *J. Biomed. Res.* 28 (2014) 435-446.
- [6] S. Thompson, B. Ballard, Z. Jiang, E. Revskaya, N. Sisay, W.H. Miller, C.S. Cutler, E. Dadachova, L.C. Francesconi, 166Ho and 90Y labeled 6D2 monoclonal antibody for targeted radiotherapy of melanoma: comparison with 188Re radiolabel, *Nucl. Med. Biol.* 41 (2014) 276-281.
- [7] F. Gao, W. Sihver, C. Jurischka, R. Bergmann, C. Haase-Kohn, B. Mosch, J. Steinbach, D. Carta, C. Bolzati, A. Calderan, J. Pietzsch, H.J. Pietzsch, Radiopharmacological characterization of ⁶⁴Cu-labeled α -MSH analogs for potential use in imaging of malignant melanoma, *Amino Acids.* 48 (2016) 833-847.
- [8] H.J. Kim, D.Y. Kim, J.H. Park, S.D. Yang, M.G. Hur, J.J. Min, K.H. Yu, Synthesis and characterization of a (68)Ga-labeled N-(2-diethylaminoethyl)benzamide derivative as potential PET probe for malignant melanoma, *Bioorg. Med. Chem.* 20 (2012) 4915-4920.
- [9] H.J. Kim, D.Y. Kim, J.H. Park, S.D. Yang, M.G. Hur, J.J. Min, K.H. Yu, Synthesis and evaluation of a novel 68Ga-labeled DOTA-benzamide derivative for malignant melanoma imaging, *Bioorg. Med. Chem. Lett.* 22 (2012) 5288-5292.

- [10] B.S. Larsson, Interaction between chemicals and melanin, *Pigment Cell Res.* 6 (1993) 127-133.
- [11] S.Y. Wu, S.P. Huang, Y.C. Lo, R.S. Liu, S.J. Wang, W.J. Lin, C.C. Shen, H.E. Wang, Synthesis and preclinical characterization of [18F]FPBZA: a novel PET probe for melanoma, *Biomed. Res. Int.* (2014) 912498.
- [12] K.P. Zhernosekov, D.V. Filosofov, R.P. Baum, P. Aschoff, H. Bihl, A.A. Razbash, M. Jahn, M. Jennewein, F. Rösch, Processing of generator-produced ⁶⁸Ga for medical application, *J. Nucl. Med.* 48 (2007) 1741-1748.
- [13] S. Liu, Bifunctional coupling agents for radiolabeling of biomolecules and target-specific delivery of metallic radionuclides, *Adv. Drug Deliv. Rev.* 60 (2008) 1347-1370.
- [14] D. Brasse, A. Nonat, Radiometals: towards a new success story in nuclear imaging?, *Dalton Trans.* 44 (2015) 4845-4858.
- [15] K.P. Eisenwiener, M.I. Prata, I. Buschmann, H.W. Zhang, A.C. Santos, S. Wenger, J.C. Reubi, H.R. Mäcke, NODAGATOC, a new chelator-coupled somatostatin analogue labeled with [^{67/68}Ga] and [¹¹¹In] for SPECT, PET, and targeted therapeutic applications of somatostatin receptor (hsst2) expressing tumors. *Bioconjug. Chem.* 13 (2002) 530-541.
- [16] R. Chakravarty, S. Chakraborty, A. Dash, M.R. Pillai, Detailed evaluation on the effect of metal ion impurities on complexation of generator eluted ⁶⁸Ga with different bifunctional chelators, *Nucl. Med. Biol.* 40 (2013) 197-205.
- [17] C.H. Taliaferro, A.E. Martell, New multidentate ligands. Xxvi. N,N'-bis(2-hydroxybenzyl)ethylenediamine-N,N'-bis(methylenephosphonic acid monomethyl ester), and N,N'-bis(2-hydroxybenzyl)ethylenediamine-N,N'-bis(methylenephosphonic acid monoethyl ester): New chelating ligands for trivalent metal ions, *J. Coord. Chem.* 13 (1984) 249-264.
- [18] M. Eder, B. Wangler, S. Knackmuss, F. Legall, M. Little, U. Haberkorn, W. Mier, M. Eisenhut, Tetrafluorophenolate of HBED-CC: A versatile conjugation agent for ⁶⁸Ga-

- labeled small recombinant antibodies, *Eur. J. Nucl. Med. Mol. Imaging.* 35 (2008) 1878–1886.
- [19] J. Schuhmacher, G. Klivenyi, R. Matys, M. Stadler, T. Regiert, H. Hauser, J. Doll, W. Maier-Borst, M. Zoller, Multistep tumor targeting in nude mice using bispecific antibodies and a gallium chelate suitable for immunoscintigraphy with positron emission tomography, *Canc. Res.* 55 (1995) 115–123.
- [20] M. Eder, M. Schafer, U. Bauder-Wust, W.E. Hull, C. Wangler, W. Mier, U. Haberkorn, M. Eisenhut, ^{68}Ga -complex lipophilicity and the targeting property of a urea-based PSMA inhibitor for PET imaging, *Biocon. Chem.* 23 (2012) 688–697.
- [21] I. Kertész, A. Vida, G. Nagy, M. Emri, A. Farkas, A. Kis, J. Angyal, N. Dénes, J. P. Szabó, T. Kovács, P. Bai, G. Trencsényi, In Vivo Imaging Of Experimental Melanoma Tumors Using The Novel Radiotracer ^{68}Ga -NODAGA-Procaïnamide (PCA), *J. Cancer.* 8 (2017) 774-785.
- [22] I. Velikyan, Prospective of ^{68}Ga -radiopharmaceutical development, *Theranostics.* 4 (2013) 47–80.
- [23] I. Velikyan, Continued rapid growth in (^{68}Ga) Ga applications: update 2013 to June 2014., *J. Labelled Comp. Radiopharm.* 58 (2015) 99-121.
- [24] D.L. Smith, W.A. Breeman, J. Sims-Mourtada, The untapped potential of Gallium ^{68}Ga -PET, the next wave of ^{68}Ga -agents, *Appl. Radiat. Isot.* 76 (2013) 14–23.
- [25] M. Eder, O. Neels, M. Müller, U. Bauder-Wüst, Y. Remde, M. Schäfer, U. Hennrich, M. Eisenhut, A. Afshar-Oromieh, U. Haberkorn, K. Kopka, Novel Preclinical and Radiopharmaceutical Aspects of [^{68}Ga]Ga-PSMA-HBED-CC: A New PET Tracer for Imaging of Prostate Cancer, *Pharmaceuticals (Basel).* 7 (2014) 779-796.
- [26] S.J. Griffin, J.B. Houston, Prediction of in vitro intrinsic clearance from hepatocytes: comparison of suspensions and monolayer cultures, *Drug Metab. Dispos.* 33 (2005) 115-120.
- [27] H.L. Mueller, R.A. Guilmette, B.A. Muggenburg, Uptake of inert particles by dog alveolar macrophages in vitro--a comparison of monolayer and suspension techniques, *J. Appl. Toxicol.* 9 (1989) 135-143.

- [28] N. Moins, J. Papon, H. Seguin, D. Gardette, M.F. Moreau, P. Labarre, M. Bayle, J. Michelot, J.C. Gramain, J.C. Madelmont, A. Veyre, Synthesis, characterization and comparative biodistribution of a new series of p-Iodine-125 benzamides as potential melanoma imaging agents, *Nucl. Med. Biol.* 28 (2001) 799-808.
- [29] M. Wolf, U. Bauder-Wüst, A. Mohamed, F. Schönsiegel, W. Mier, U. Haberkorn, M. Eisenhut, Alkylating benzamides with melanoma cytotoxicity, *Melanoma Research.* 14 (2004) 353-360.
- [30] M. Wolf, U. Bauder-Wüst, U. Haberkorn, W. Mier, M. Eisenhut, Alkylating benzamides with melanoma cytotoxicity: role of melnon, tyrosinase, intracellular pH and DNA interaction, *Melanoma Research.* 15 (2005) 383-391.
- [31] G. Ren, Z. Miao, H. Liu, L. Jiang, N. Limpa-Amara, A. Mahmood, S.S. Gambhir, Z. Cheng, Melanin-targeted preclinical PET imaging of melanoma metastasis, *J. Nucl. Med.* 50 (2009) 1692-1699.
- [32] L. Lattuada, A. Barge, G. Cravotto, G.B. Giovenzana, L. Tei, The synthesis and application of polyamino polycarboxylic bifunctional chelating agents, *Chem. Soc. Rev.* 40 (2011) 3019-3049.
- [33] L.A. Bass, M. Wang, M.J. Welch, C.J. Anderson, In vivo transchelation of copper-64 from TETA-octreotide to superoxide dismutase in rat liver, *Bioconjug. Chem.* 11 (2000) 527-532.
- [34] A. E. Martell, R. J. Motekaitis, E. T. Clarke, R. Delgado, Y. Sun, R. Ma, Stability constants of metal complexes of macrocyclic ligands with pendant donor groups, *Supramol. Chem.* 6 (1996) 353-363.
- [35] A. Harrison, C.A. Walker, D. Parker, K.J. Jankowski, J.P. Cox, A.S. Craig, J.M. Sansom, N.R. Beeley, R.A. Boyce, L. Chaplin, The in vivo release of ⁹⁰Y from cyclic and acyclic ligand-antibody conjugates, *Int. J. Rad. Appl. Instrum. B.* 18 (1991) 469-476.

- [36] J.B. Stimmel, M.E. Stockstill, F.C. Jr. Kull, Yttrium-90 chelation properties of tetraazatetraacetic acid macrocycles, diethylenetriaminepentaacetic acid analogues, and a novel terpyridine acyclic chelator, *Bioconjug. Chem.* 6 (1995) 219-225.

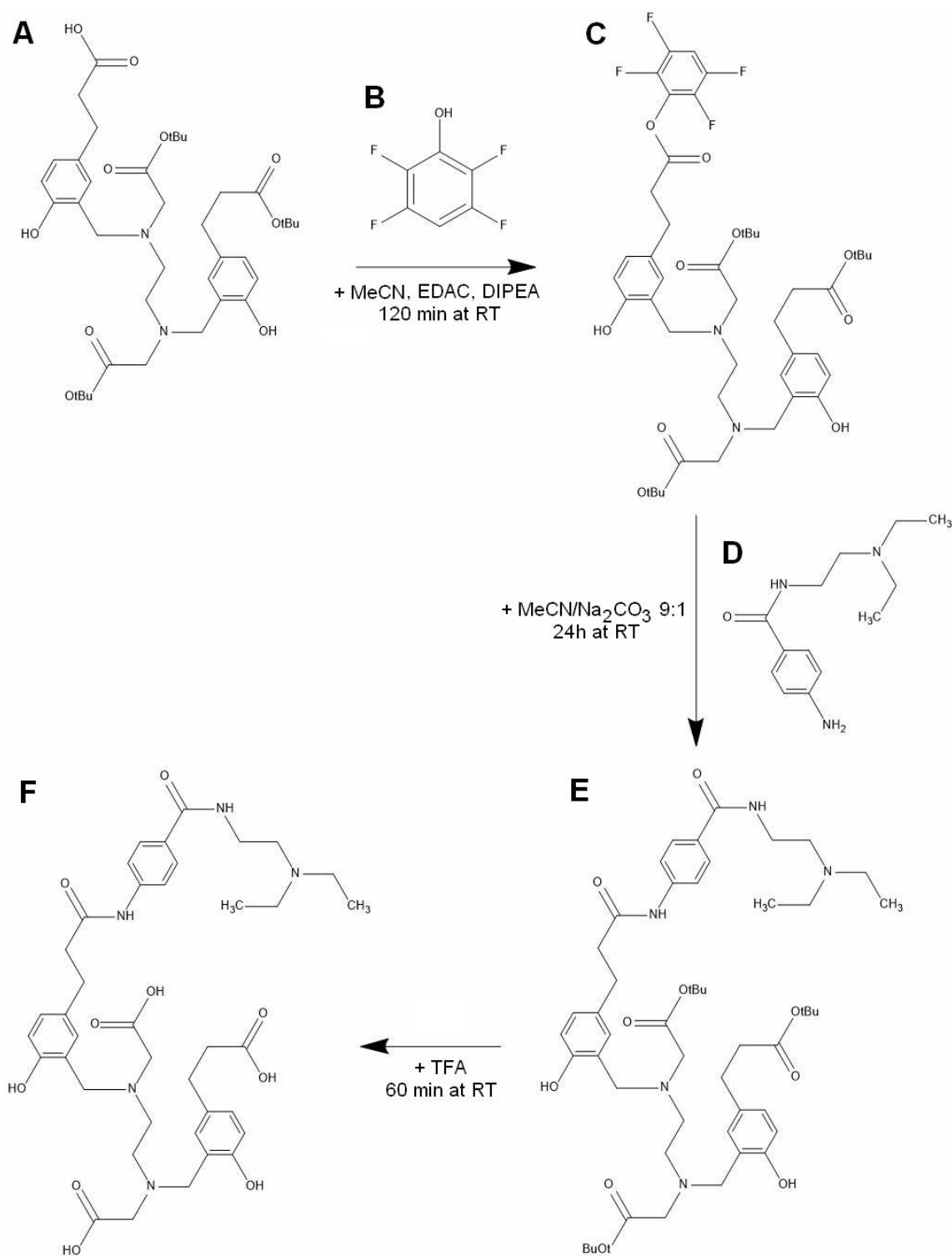


Fig. 1. The reaction scheme of the chemical synthesis of HBED-CC-PCA. A: N,N'-Bis[2-hydroxy-5-(carboxyethyl)-benzyl]ethylenediamine-N,N'-diacetic acid, tris tert-butyl ester (HBED-CC-tris(tBu)ester); B: 2,3,5,6-tetrafluorophenol; C: HBED-CC-tris(tBu) tetra-fluoro-phenyl ester; D: 4-amino-N-(2-diethylaminoethyl)benzamide hydrochloride; E: HBED-CC-tris(tBu)ester-PCA; F: HBED-CC-PCA.

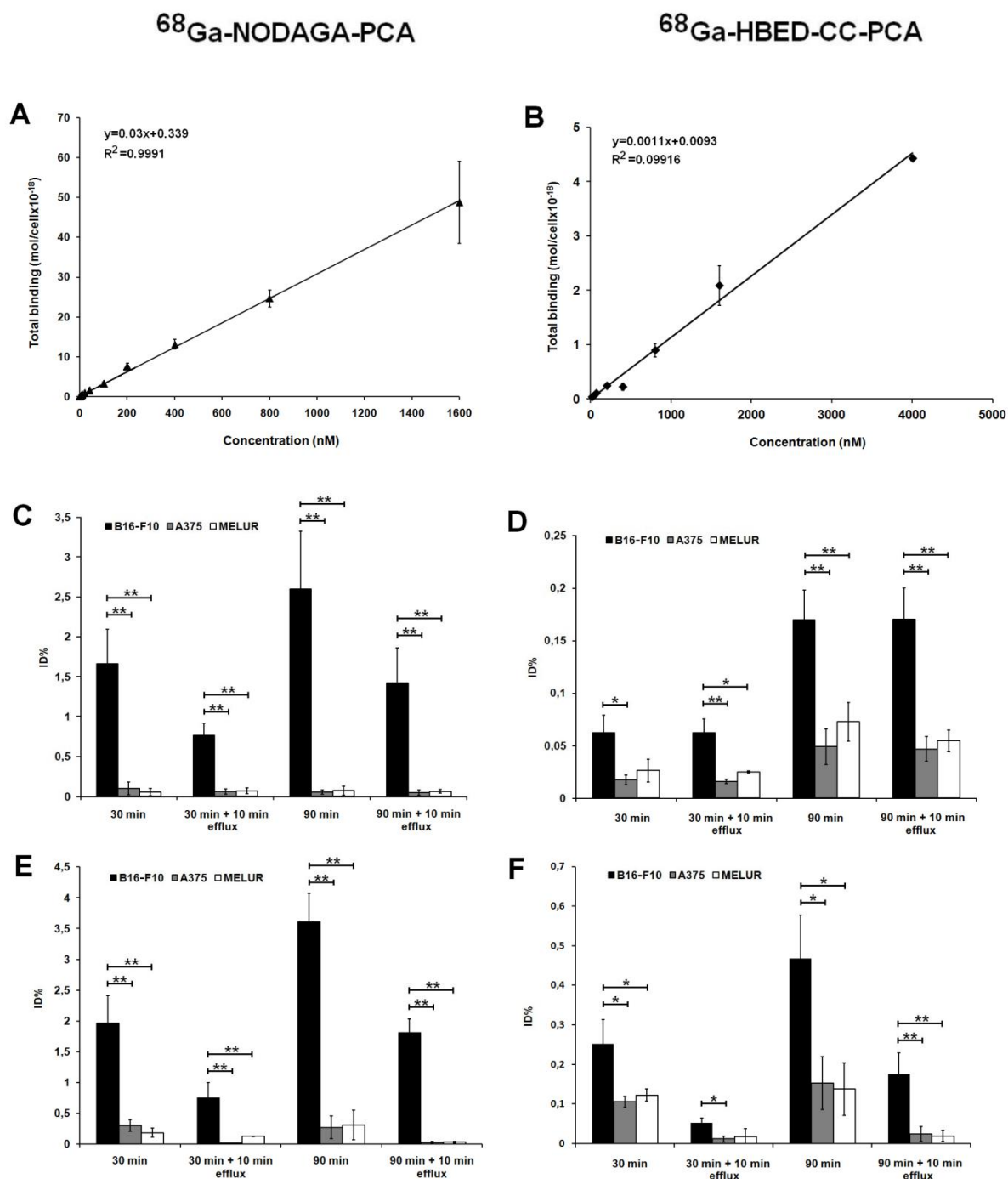


Fig. 2. Assessment of cellular binding, uptake and efflux studies of melanin specific ^{68}Ga -NODAGA-PCA and ^{68}Ga -HBED-CC-PCA. *In vitro* saturation binding studies in B16-F10 cells incubated with different concentrations of ^{68}Ga -NODAGA-PCA (A) and ^{68}Ga -HBED-CC-PCA (B) at 37 °C for 1 h. Comparison of time dependent ^{68}Ga -NODAGA-PCA (C, E) and ^{68}Ga -HBED-CC-PCA (D, F) uptake and washout (efflux) results of B16-F10, A375 and Melur cells measured in suspension (C, D) and monolayer (E, F). Significance level: $p \leq 0.05$

(*), $p \leq 0.01$ (**). The data values shown are means \pm SD of the results of at least three independent experiments, each performed in triplicate. ID%: Tracer accumulation in 10^6 cells was expressed as the percentage of the incubating dose.

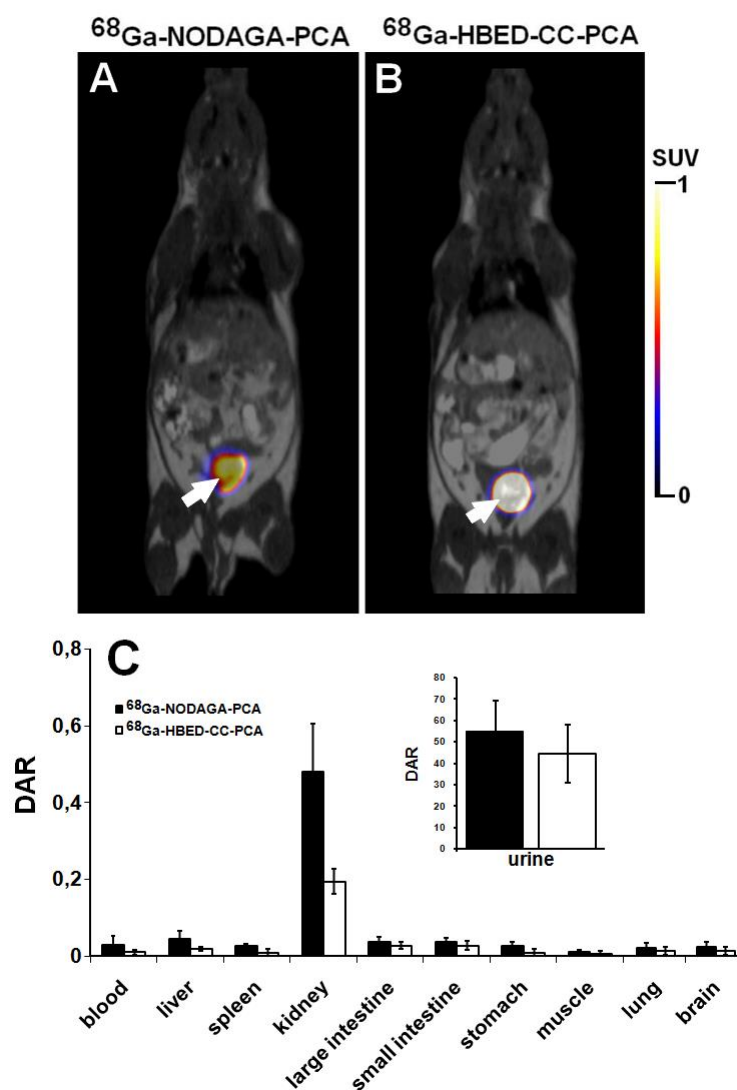


Fig. 3. *In vivo* and *ex vivo* biodistribution data for ^{68}Ga -NODAGA-PCA. A: Representative coronal microPET/MRI image of healthy control C57BL/6 mouse 90 min after the radiotracer injection. Yellow arrow: liver; red arrows: kidneys; white arrow: bladder with urine. B: quantitative analysis of tracer uptake in control animals (n=5) 90 min after the injection of ^{68}Ga -NODAGA-PCA. DAR values are presented as mean \pm SD.

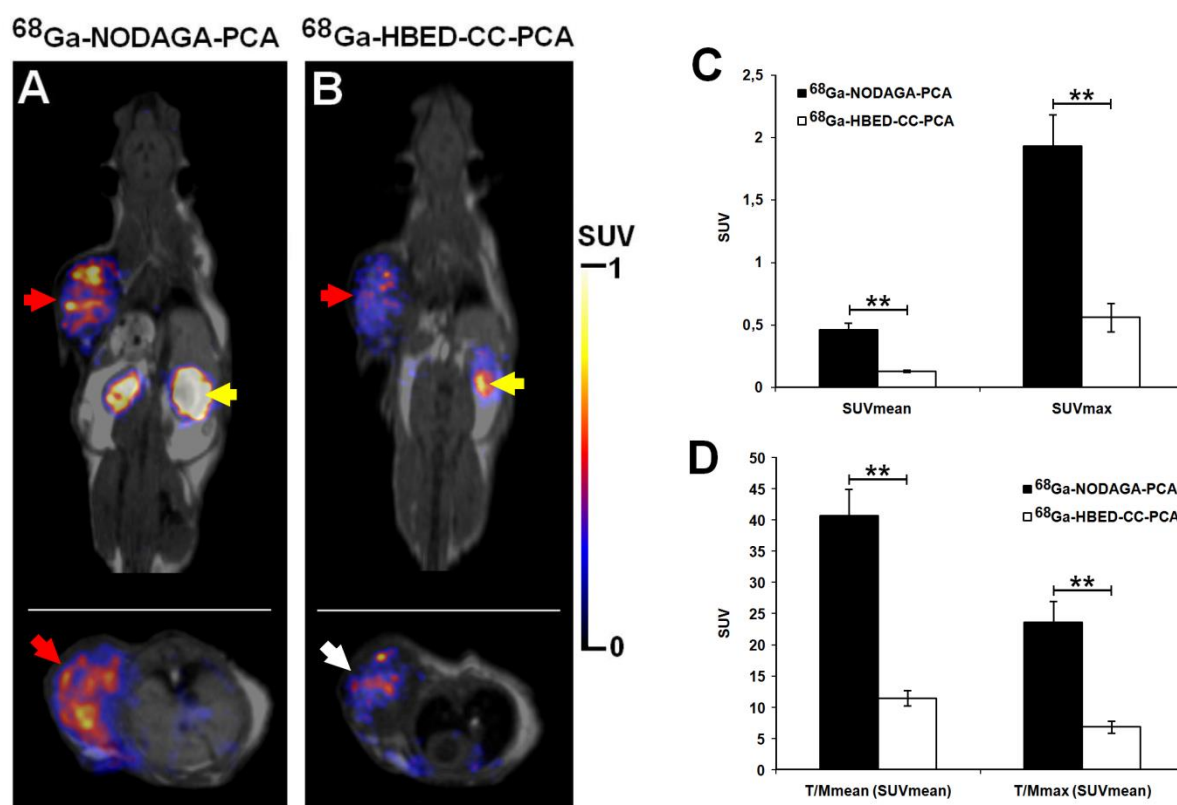


Fig. 4. Representative whole body coronal (A and B: upper row) and axial (A and B: lower row) nanoScan PET/MRI images of the same B16-F10 melanoma tumor-bearing C57BL/6J mouse 21 days after tumor cell inoculation and 90 min after intravenous injection of ^{68}Ga -NODAGA-PCA (A, red arrows) and ^{68}Ga -HBED-CC-PCA (B, white arrows). Yellow arrows: kidney. Quantitative SUV analysis of ^{68}Ga -NODAGA-PCA (n=10) and ^{68}Ga -HBED-CC-PCA (n=10) accumulation in B16-F10 tumors (C) and tumor-to-muscle ratios (D). Significance level: $p \leq 0.01$ (**). SUV: standardized uptake value; T/M: tumor-to-muscle ratio.

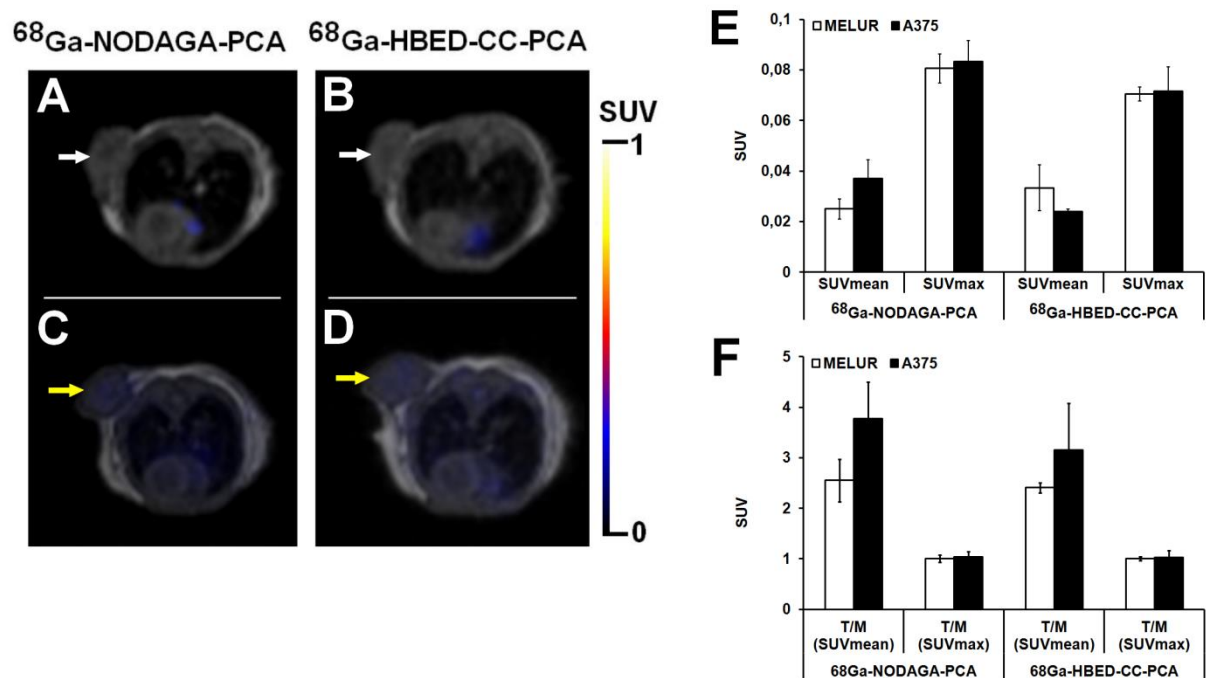


Fig. 5. *In vivo* assessment of radiotracer accumulation in melanin negative tumors. Representative axial PET/MRI images of MELUR (A, B; white arrows) and A375 (C, D; yellow arrows) melanoma tumor-bearing SCID mice 23 days after tumor cell injection and 90 min after intravenous injection of ^{68}Ga -NODAGA-PCA (A, C) or ^{68}Ga -HBED-CC-PCA (B, D). Quantitative SUV analysis of ^{68}Ga -NODAGA-PCA (n=10) and ^{68}Ga -HBED-CC-PCA (n=10) uptake in melanin-negative tumors (E) and tumor-to-muscle ratios (F). Significance level: $p \leq 0.01$ (**). SUV: standardized uptake value; T/M: tumor-to-muscle ratio.

Table 1: ^{68}Ga -NODAGA-PCA and ^{68}Ga -HBED-CC-PCA accumulation (DAR) in *s.c.* B16-F10, A375 and MELUR tumors 90 min after tracer injection and 21 ± 2 days after tumor cell inoculation. Significance level between melanotic B16-F10 and amelanotic (A375, MELUR) tumors using ^{68}Ga -NODAGA-PCA: $p\leq 0.01$ (**) and ^{68}Ga -HBED-CC-PCA: $p\leq 0.05$ (*)

Tumor	^{68}Ga-NODAGA-PCA	^{68}Ga-HBED-CC-PCA
B16-F10 tumor (n=5)	$0.42 \pm 0.07^{**}$	$0.13 \pm 0.03^*$
B16-F10 tumor/muscle	$23.64 \pm 2.73^{**}$	$8.05 \pm 0.99^*$
A375 tumor	0.06 ± 0.02	0.03 ± 0.01
A375 tumor/muscle	1.85 ± 0.25	1.62 ± 0.18
MELUR tumor	0.04 ± 0.01	0.02 ± 0.01
MELUR tumor/muscle	1.32 ± 0.19	1.11 ± 0.09